Forward Jet and Hadron Production at Low x and Q^2

Timothy Greenshaw

Oliver Lodge Laboratory, Liverpool University, Liverpool L69 7ZE, ENGLAND

Abstract. Recent measurements of forward jet and single forward hadron production at HERA are described. An introduction is given to some of the consequences of various QCD approximation schemes used in the calculation of forward jet and particle production cross sections.

1 Introduction

1.1 HERA measurements and QCD

The H1 and ZEUS experiments at the HERA electron-proton (ep) collider have made impressive progress since HERA delivered first luminosity in 1992. Measurements of many aspects of ep interactions have been made with high precision over a large kinematic range. Here, we concentrate on measurements of jet and particle production in the forward region[1] and the description of these measurements provided by QCD. We shall work in the deep-inelastic scattering (DIS) regime, the regime in which both the negative squared four-momentum transferred to the proton from the electron $Q^2 = -q^2 \gg m_p^2$ and the final state hadronic mass squared $W^2 \gg m_p^2$, where m_p is the mass of the proton. Figure 1 illustrates the definition of some of these variables. For the measurements discussed here $Q^2 \ll m_Z^2$, where m_Z is the Z^0 mass, so the interactions can be considered to be mediated by virtual photons. In addition $W^2 \gg Q^2$, so the Bjorken scaling variable $x = Q^2/(Q^2 + W^2) \ll 1$. Recall that, in the frame in which the proton has infinite momentum, x is the fraction of the proton's momentum carried by the quark struck in the deep-inelastic interaction.

The HERA data are, on the whole, described extremely well by QCD. For example, the dijet cross section measurements presented in [1] are beautifully reproduced by NLO QCD calculations.

1.2 First forward jet measurements

If we now move to consider explicitly the forward region, the above no longer holds; NLO QCD [4] fails to describe the first HERA forward jet cross section measurements [2], as shown in figure 2. What is happening here?

[1] The HERA co-ordinate system has its origin at the nominal interaction point, its z axis in the proton direction and its y axis vertical; the x axis completes the right-handed orthogonal co-ordinate system. Polar angles are denoted by θ and azimuthal angles by ϕ. The term "forward" refers to the region for which $\theta < 90°$.

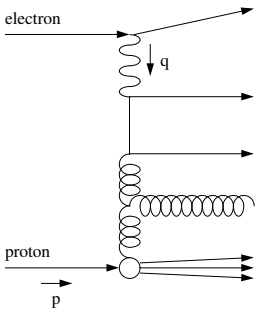

Fig. 1. A generic Feynman diagram for deep-inelastic ep scattering, illustrating the definition of some of the commonly used variables.

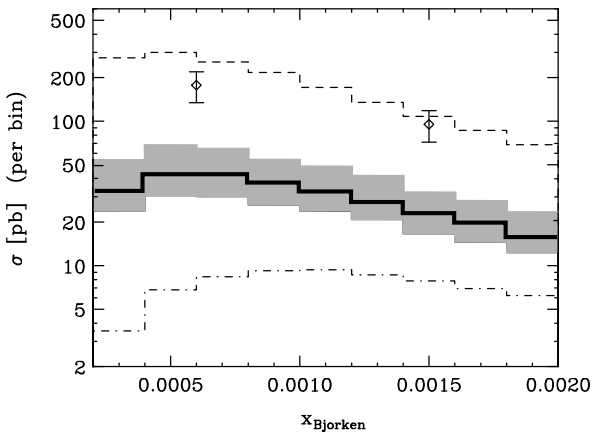

Fig. 2. The forward jet cross section in the kinematic regon described the text. The error bars illustrate the quadratic sum of the statistical and the systematic errors. The curves show NLO QCD calculations with an error band corresponding to a scale variation of two orders of magnitude, LO QCD calculations and the results of a BFKL calculation.

The key to understanding the problem lies in the definition of the kinematic region in which the forward jet measurement was made; it was required that the squared transverse momentum of the jet be similar to Q^2, $0.5 < p^2_{T\mathrm{jet}}/Q^2 < 4$, and that the jets have a large longitudinal momentum in the proton direction. This latter condition arises from the requirements that the jets be found in the forward region, $6° < \theta_{\mathrm{jet}} < 20°$, and that the ratio $x_{\mathrm{jet}} = E_{\mathrm{jet}}/E_p > 0.025$, Here, E_{jet} and E_p are the jet and proton energies, respectively. Hence, the parton emitted from the proton which caused the production of the forward jet must have carried a large proportion of the proton's momentum, and yet the quark

struck by the virtual photon carried only a very small proportion of the proton's momentum, as the Bjorken x range considered was $2 \times 10^{-4} < x < 2 \times 10^{-3}$. The diagram in figure 1 may well be misleading. The phase space for the parton emerging from the proton to emit further partons is particularly large in this case, so the situation could be more like that illustrated in figure 3. Calculating

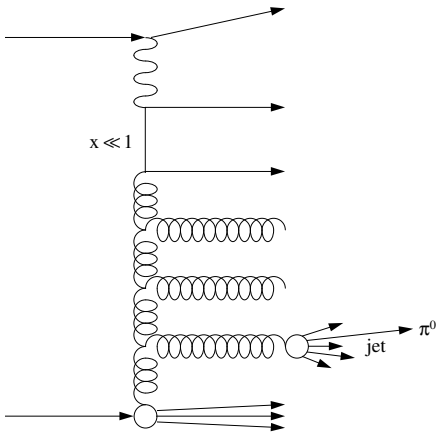

Fig. 3. A Feynman diagram illustrating low x DIS with the production of a forward jet carrying a large proportion of the proton's momentum, containing an energetic π^0.

to order α_s^2 allows us a maximum of 3 partons, as shown in figure 3, and such calculations are unlikely to be able to describe situations in which larger numbers of partons play a significant role. Is it possible for us to include the effects of these? Here, we use the Uncertainty Principle to try and construct an approximate picture of how we might expect these partons to behave, before going on compare the results of QCD calculations, made using various approximation schemes, to the HERA data. The calculations are discussed in more detail in other contributions to these proceedings [3].

Consider a fast parton, 1, which emits a further parton, 2, as illustrated in figure 4. The initially massless system has now acquired a mass given by:

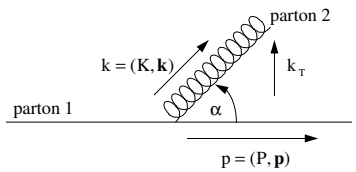

Fig. 4. A parton 1 emitting a parton 2, with four-momenta as illustrated.

$$M^2 = (p+k)^2 = 2(PK - PK\cos\alpha) \approx PK\alpha^2.$$

The magnitude of the resulting energy change, which determines the length of time the virtual system can exist before 2 is re-absorbed by 1, is $\Delta E = M$ in the rest frame of the system. Including the time dilation factor $\gamma \approx P/M$ gives the time for which this state can exist in the laboratory:

$$\begin{aligned}\Delta t &= \frac{1}{\Delta E} = \frac{1}{M}\frac{P}{M} \\ &= \frac{P}{PK\alpha^2} = \frac{1}{K\alpha^2}.\end{aligned}$$

Using the fact that $\alpha \approx k_T/K$ we have $\Delta t \approx K/k_T^2$. Such emissions and re-absorptions will take place continuously in a proton prior to a deep-inelastic interaction. The interaction will "free" all the partons that exist at the time it takes place. We see that there will be some which can have existed for a long time before the interaction, those with large $\Delta t \approx K/k_T^2 \approx k_L/k_T^2$, and others that can only have existed for a very short time before the interaction, those with small $\Delta t \approx k/k_T^2$; it will appear that there is shower of time ordered partons $1, 2, 3 \ldots$ such that $K_1/k_{T1}^2 > K_2/k_{T2}^2 > K_3/k_{T3}^2 \ldots$

1.3 The DGLAP, BFKL and CCFM equations

The above argument suggests that we can think of the initial state partons as forming a cascade in which either the k_T increases strongly as we move towards the photon-quark vertex, with the longitudinal momentum relatively constant, or the longitudinal momentum decreases and the k_T remains approximately constant. A further alternative is to consider there to be an ordering of the emission angles[2], as illustrated in figure 5. These three possibilities correspond

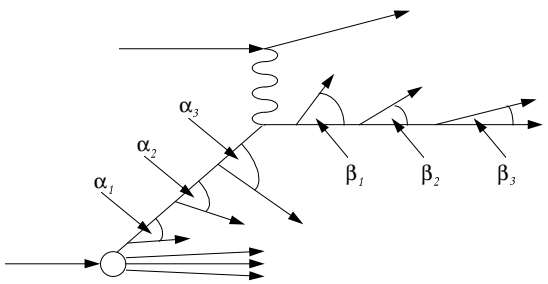

Fig. 5. Angular ordering in initial and final state parton cascades.

roughly to three approximation schemes within QCD which allow the inclusion

[2] For completeness sake, note that the emissions in the final state occur in order of decreasing angle.

of the effects of certain terms in the perturbative expansion of DIS processes to all orders. The case in which the cascade is considered as being composed of partons strongly ordered in k_T, $k_{T1}^2 \ll k_{T2} \ll k_{T3}^2 \ldots$, corresponds to using the Dokshitzer, Gribov, Lipatov, Altarelli and Parisi (DGLAP) equations [5], which sum to all orders, n, the terms $\sim \log^n Q^2$. How this is done is discussed in [6]. The case in which the cascade is considered to be composed of partons with decreasing longitudinal momenta, $x_1 \gg x_2 \gg x_3 \ldots$, corresponds to using the Balitski, Fadin, Kadeev and Lipatov equations [7], which are discussed in [8]. These sum to all orders the terms $\sim \log^n(1/x)$. Thinking of the partons as being ordered in emission angle, $\alpha_1 < \alpha_2 < \alpha_3 \ldots$, corresponds to using the Ciafaloni, Catani, Fiorani and Marchesini (CCFM) equations [9].

The success of the DGLAP equations is well known. For example, they give an excellent description of HERA $F_2(x, Q^2)$ measurements despite the range of more than four orders of magnitude in both Q^2 and x spanned by the HERA data, as is discussed in [10]. Can they describe the forward jet measurements? Looking at the kinematic region chosen, we must conclude that it is unlikely. The DGLAP equations describe data in which the parton cascade can be thought of as being ordered in k_T, the forward jet measurement, in which it is required that $k_{T\text{jet}}^2 \sim Q^2$ precludes the development of such cascades as the k_T at both ends of the cascade is similar. Figures 7, 8a) and 8c) confirm our suspicions.

Let us turn instead to the BFKL equation. This should give accurate results where the cascade can be thought of as consisting of partons with strongly decreasing longitudinal momenta. This is exactly the situation here. The requirement that x_{jet} be large and x small ensures that the longitudinal momentum at the start of the cascade is large and that at the end small. Indeed, this is precisely the reason why these conditions were chosen for the measurement [11], the hope being that a kinematic region could be found in which there was clear evidence for the applicability of the BFKL equation. The evidence from the early forward jet measurements, as shown in figure 2, is that the BFKL solution [12] does a good job.

1.4 Monte Carlo Programs

Monte Carlo (MC) programs provide an alternative means of comparing QCD calculations with measurements. The programs of interest here are the following:

- LEPTO [13] matches LO QCD matrix elements with DGLAP inspired parton showers; the showers display k_T ordering.
- RAPGAP [14], originally developed to simulate diffractive DIS events, is very similar to LEPTO; the facility to simulate the effects of allowing the virtual photon to develop hadronic structure is of interest here, as is discussed in the following.
- HERWIG [15] produces DGLAP-like showers using angular ordering. The showers are corrected to incorporate the correct LO QCD results for the photon-parton interaction.

- ARIADNE [16] is an implementation of the Colour Dipole Model [17] (CDM), which treats QCD radiation as arising from the colour dipole generated in the deep-inelastic scattering process; the resulting parton cascades do not display k_T ordering and in this sense the results of the CDM are similar to those of the BFKL equation.
- The Linked Dipole Chain [18] (LDC) model relies on a re-formulation of the CCFM equations and should produce DGLAP-like and BFKL-like showers in the appropriate high Q^2 and low x limits, or, more accurately in the situations in which there is a large k_T or x "lever arm", respectively. It has been shown that, at the level of the leading log (LL) terms $\sim \log^n(1/x)$, the predictions of the CCFM equations for the hadronic final state in DIS at small x are identical to those of the BFKL equation [19].

One advantage of using MCs to compare theoretical predictions with data is that the MCs incorporate hadronisation models. This allows direct comparison of the predictions with data; parton level jet cross sections are likely to differ by 15 to 20% from the results expected following hadronisation. All the above models, barring HERWIG, use the JETSET [20] implementation of colour string fragmentation to perform hadronisation, following their various parton cascade schemes. The HERWIG model forms low mass colourless "pre-clusters" following its cascade procedure. These are then allowed to decay into hadrons.

2 New forward jet measurements and BFKL calculations

The H1 and ZEUS Collaborations have both produced new forward jet measurements since those discussed above. Both groups used a "cone" algorithm to identify the jets in the laboratory frame of reference. These algorithms maximise the transverse energy within a cone of radius $\sqrt{\Delta\eta^2 + \Delta\phi^2} = 1$, where $\Delta\eta$ is the difference in pseudorapidity, $\eta = -\ln(\tan(\theta/2))$, between the cone's axis and the calorimeter energy deposits under consideration, and $\Delta\phi$ is the difference in azimuthal angle. The algorithm used by ZEUS is described in [21]. The ZEUS measurement requires in addition that $x'_{\rm jet} = p_{z\rm jet}/E_p > 0.036$, $0.5 < E^2_{T\rm jet}/Q^2 < 2$, $\eta_{\rm jet} < 2.6$ (*i.e.* $\theta_{\rm jet} > 8.5°$) and that $E_{T\rm jet} > 5\,\mathrm{GeV}$. Further, to explicitly remove events in which the forward jet is caused by the quark scattered in the deep-inelastic interaction, ZEUS require that the longitudinal momentum of the jet in the Breit frame of reference[3] $p^{\rm Breit}_{z\rm jet} > 0$. The Bjorken x region studied is $4.5 \times 10^{-4} < x < 4.5 \times 10^{-2}$. Despite the experimental difficulties involved in making this measurement, particularly the problems of measuring energy deposits close to the outgoing proton remnant and the forward beamhole in the calorimeter, the distribution of transverse energy about the forward jet axis following the above selection does reveal jet structure, as is illustrated in figure 6.

[3] The Breit frame is the frame of reference in which the four-momenta of the virtual photon and the proton are given by $(E, p_T, p_L) = (0, 0, -Q)$ and $(Q/2x, 0, Q/2x)$, respectively.

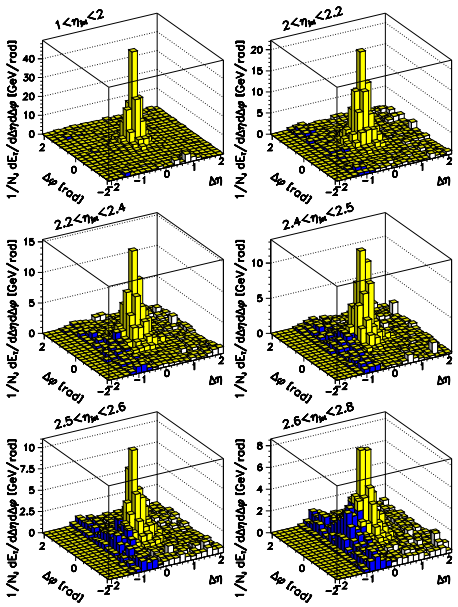

Fig. 6. The transverse energy flow around the forward jet axis averaged over all forward jets for various $\eta_{\rm jet}$ regions; grey indicates the E_T attributed to the jet, black the E_T around the calorimeter beam hole and white other E_T deposits.

Figure 7 shows the forward jet cross section [22] obtained by the ZEUS Collaboration[4]. Also shown in figure 7 are the predictions of several MC programs. Neither the DGLAP based MCs, LEPTO and HERWIG, nor the LDC MC are able to describe the data. The "pseudo-BFKL" MC prediction, that of ARIADNE, is the best of those shown.

The new H1 forward jet measurements [23] are shown in figure 8. The cone algorithm used here is described in [24]. The requirements made on the forward jets were that $x_{\rm jet} > 0.035$, $0.5 < p^2_{T\rm jet}/Q^2 < 2$ and $7^\circ < \theta_{\rm jet} < 20^\circ$. Results are shown in two regions of $p_{T\rm jet}$, namely $p_{T\rm jet} > 3.5\,\mathrm{GeV}$ and $p_{T\rm jet} > 5\,\mathrm{GeV}$. As in the above case, all MC predictions fall below the data, including those of the LDC model, with ARIADNE providing the best description of the data. NLO QCD calculations are again seen to fall significantly below the data, with a LO BFKL calculation tending to be too high. The discrepancy between the latter calculation and the LDC MC is intriguing given the formal equivalence of the CCFM and BFKL equations at the LL level. Are there significant sub-leading terms? Have we still to reach "low" x?

[4] In this and subsequent figures in which experimental data are shown, the inner error bars correspond to the statistical errors, the outer error bars to the quadratic sum of the statistical and systematic errors.

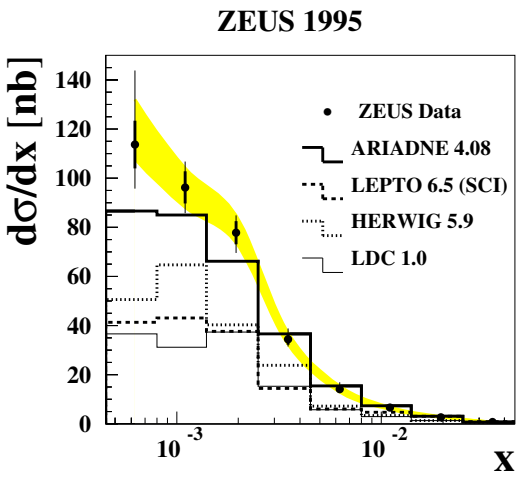

Fig. 7. The forward jet cross section as a function of x in the kinematic region described in the text with the additional requiremnts that the scattered electron energy $> 10\,\mathrm{GeV}$ and that $y > 0.1$. The curves show the predictions of various MC programs.

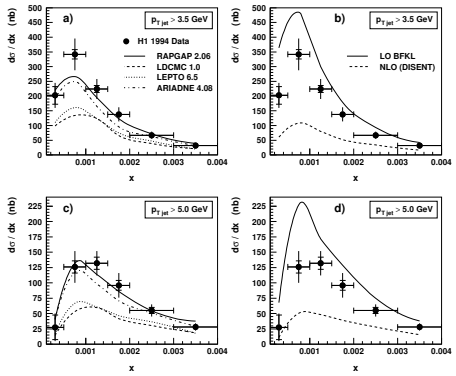

Fig. 8. The forward jet cross section as a function of x for $p_{T\mathrm{jet}} > 3.5\,\mathrm{GeV}$ and $p_{T\mathrm{jet}} > 5\,\mathrm{GeV}$; the curves in a) and c) are MC predictions, in b) and d) the full lines are analytic LO BFKL calculations without inclusion of the effects of the jet algorihm, the dashed lines are NLO QCD calculations made using DISENT [25] and include the effects of the jet algorithm at the parton level.

As mentioned above, and described in more detail in [26], the BFKL results used to this point rely on a summation of the LL terms. Recently, a calculation of the effects of the next-to-leading log (NLL) terms, $\sim \log^{n-1}(1/x)$, has become available [27] which has showed that they can be as large as the effects of the LL terms. The resulting debate on whether and how, despite this, BFKL-based

phenomenology may be possible has yet to be resolved [28–30][5]. Here, we consider modified LL BFKL calculations, incorporating a "consistency constraint" which effectively includes part of the NLL terms [32]. The forward jet cross section determined using this approach is shown in figure 9, for various choices of scale, with the forward jet measurements of the ZEUS and H1 Collaborations. The

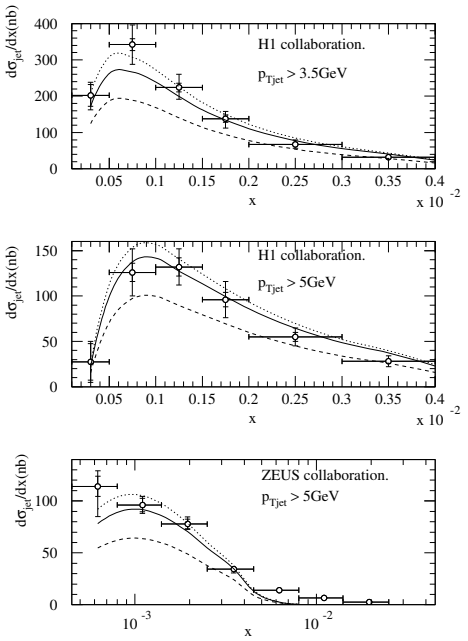

Fig. 9. The forward jet cross section measurements of ZEUS and H1 as a function of x compared with BFKL calculations including a "consistency constraint", for various choices of scale.

modified LL BFKL calculation is significantly better than the unadulterated LL BFKL result shown in figure 8.

The H1 forward dijet rates, measured in the kinematic range given above with the requirement that both jets satisfy $p_{T\mathrm{jet}} > 3.5\,\mathrm{GeV}$, is $\sigma_{2\mathrm{jet}} = 6.0 \pm 0.8\,(\mathrm{stat.}) \pm 3.2\,(\mathrm{syst.})\,\mathrm{pb}$, which compares favourably with the prediction from the modified BFKL calculations of $\sigma_{2\mathrm{jet}} = 2.7 \ldots 5.2\,\mathrm{pb}$, where the range results from varying the choice of scale.

[5] For discussion of the problems associated with the running of α_S in the BFKL formalism see, for example, [31]

3 Forward particle production

A problem that arises when trying to compare forward jet measurements with BFKL based calculations is the uncertainty of 15 to 20% introduced by the effect of hadronisation. This can be circumvented by comparing predictions for single forward π^0 production with measurement. Here, measured π fragmentation functions are folded with the above modified BFKL calculations [32], as illustrated in figure 3. The success of this approach is apparent in figure 10, in which the

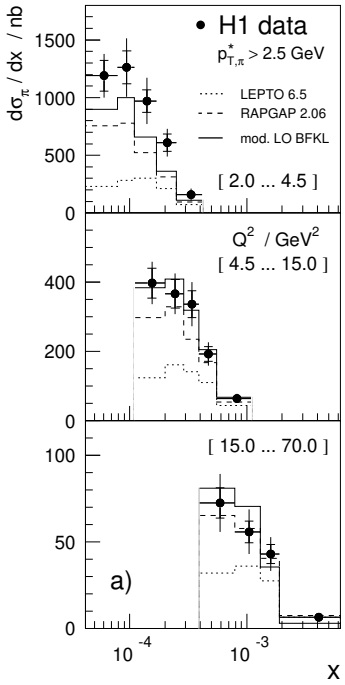

Fig. 10. The H1 forward π^0 cross section as a function of x compared with BFKL calculations including a "consistency constraint", and with two DGLAP MCs, one which allows for the effects of virtual photon structure (RAPGAP) and one which does not (LEPTO).

calculations are compared with the H1 forward π^0 measurements [33].

4 Forward jets and virtual photon structure

Intriguingly, in figure 10 it is not only the BFKL calculation that provides a reasonable description of the data, the results of the RAPGAP MC are also

respectable. RAPGAP is a DGLAP based MC, but allows for the inclusion of the effects of virtual photon structure. Such effects may become significant in the regime in which the k_T^2 at the photon end of the parton cascade exceeds the photon's virtuality Q^2. Recall that the transverse dimensions of the photon are $\sim 1/\sqrt{Q^2}$ and that the transverse wavelength of the partons $\lambda_T \sim 1/k_T$. If $\lambda_T < 1/\sqrt{Q^2}$ the parton is able to resolve the hadronic structure of the virtual photon which arises through the $\gamma \to q\bar{q}$ splitting. Indeed, such events have been used to determine the effective parton density in the virtual photon [34]. Is this relevant to forward particle and jet production? The answer is a resounding perhaps, as can be seen by the following argument. The requirement that $0.5 < p_{T\mathrm{jet}}^2/Q^2 < 2$ allows events in which $k_T > Q^2$ into the sample studied, both explicitly at the high end of the $p_{T\mathrm{jet}}^2/Q^2$ range and implicitly in that the correlation between $p_{T\mathrm{jet}}$ and k_T is far from 100%. This implies we are in a regime in which virtual photon structure may be significant. In addition, the fact that the parton entering the hard scattering process from the photon side carries only a fraction $x_\gamma = p_{\mathrm{part}}/p_\gamma$ of the momentum p_γ of the photon ensures that the resulting jets will tend to be more forward than in the situation in which $x_\gamma = 1$, as is illustrated in figure 11. In terms of parton cascades, if we choose to explain

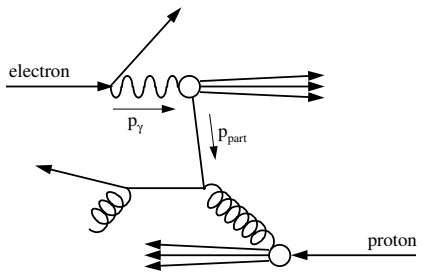

Fig. 11. A DIS event in the HERA laboratory frame in which the structure of the virtual photon is resolved leading to the production of forward jets and particles, *i.e.* jets and particles adjacent to the proton remnant.

the development of both the virtual photon structure "within" the photon and the structure within the proton using the DGLAP prescription, we will have cascades of partons with increasing k_T developing from both the photon and proton ends of the interaction, as illustrated in figure 12. Note that this picture bears some resemblance to the parton cascade produced by the ARIADNE MC, in which there is no k_T ordering. This is a possible explanation for the success of ARIADNE in describing the forward jet and forward particle measurements.

The MC predictions including the effects of virtual photon structure not only describe forward particle production but also provide a reasonable description of the forward jet results, as is shown in figure 13. In this figure comparison is made

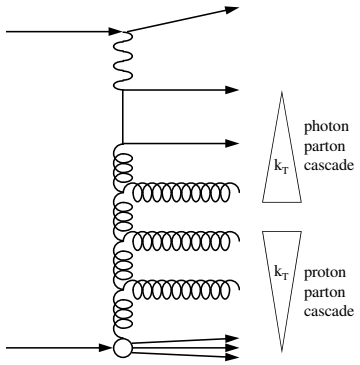

Fig. 12. An illustration of a DIS event in which the structure of both the virtual photon and the proton develops via a parton cascade described by the DGLAP prescription, with k_T ordering as indicated by the increasing width of the relevant triangles.

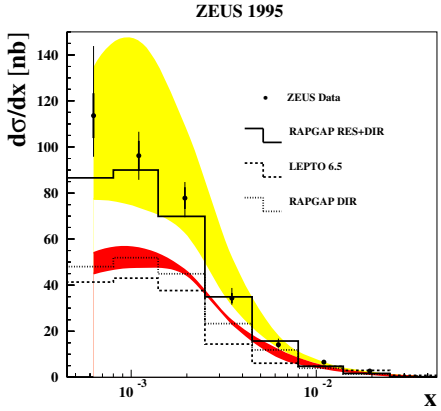

Fig. 13. The ZEUS forward jet measurements as a function of x shown with predictions from MCs with, RAPGAP RES+DIR, and without, LEPTO and RAPGAP DIR, the effects of virtual photon structure.

firstly with LEPTO and RAPGAP allowing only direct photons to contribute, that is those in which the structure of the photon is not resolved. These models are very similar, as is borne out by the results shown, and are not able to describe the data. Allowing the inclusion of resolved photon processes, those in which the partonic structure of the virtual photon is resolved, significantly improves the quality of the description.

This approach, allowing the inclusion of virtual photon structure, can also be taken in NLO QCD calculations, as is discussed in [35,36]. The results of such calculations are shown in figure 14 together with the H1 forward jet measurements. Again, the agreement is found to be good.

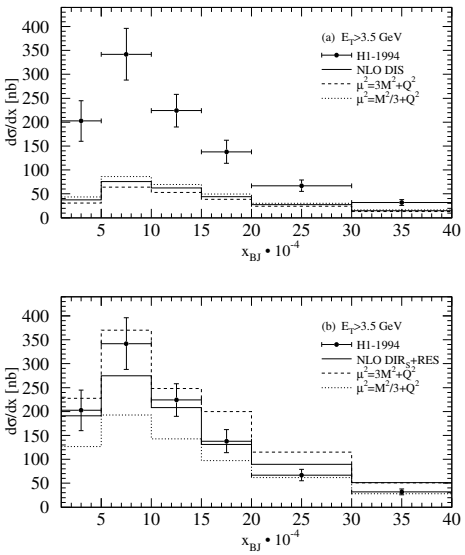

Fig. 14. The H1 forward jet measurements as a function of x shown with the results of NLO QCD calculations (a) without and (b) with the effects of virtual photon structure for various choices of scale.

5 Summary

HERA has provided new impetus to both theoretical and experimental investigations of low x QCD and recent progress has been impressive. We are now able to describe reasonably the measured rates of forward jets [23,22] using either NLO QCD calculations incorporating virtual photon structure [35], modified BFKL calculations [32] or MCs based on LO QCD allowing either directly, as in the case of RAPGAP [14], or indirectly, as in the case of ARIADNE [16], for virtual photon structure. The relative success of ARIADNE may alternatively be considered to be associated with the BFKL-like nature of the parton showers it produces. It is likely that NNLO QCD calculations will provide as good a description of data as the above without having to invoke virtual photon structure [36]. Forward π^0 production is also reasonably described within the modified BFKL framework. New low x MC programs are being developed, such as the LDC MC [18], which is based on a reformulation of the CCFM [9] equations and as such should reproduce BFKL predictions for the hadronic final state in DIS at small x [19]. Many problems remain to be solved, however. The recent calculation of the NLL corrections to the BFKL equation [27] raises difficulties associated with both the running of α_S and the unexpectedly large size of the corrections. The apparent disagreement between LDC MC predictions and LL BFKL calculations is a puzzle. Experimentally, measurements in the forward region remain a challenge. Improving the precision of current measurements and

devising new ways of testing low x QCD will tax the ingenuity of physicists for many years to come.

Acknowledgments

The author would like to thank the organisers of Ringberg 99 for the invitation to spend a week in delightful surroundings in such stimulating company. Thanks also to Dr. S.J. Maxfield for his careful reading of this manuscript.

References

1. L. Jönsson, these proceedings.
2. S. Aid *et al.* [H1 Collaboration], Phys. Lett. **B356** (1995) 118.
3. See the contributions of to these proceedings of A. Martin, J. Blümlein, E. Levin, B. Pötter, J. Outhwaite, M. Klasen and D. Graudenz.
4. E. Mirkes and D. Zeppenfeld, Phys. Rev. Lett. **78** (1997) 428.
5. Yu.L. Dokshitzer, Sov. Phys. JETP **46** (1977) 641;
   V.N. Gribov and L.N. Lipatov, Sov. J. Nucl. Phys. **15** (1972) 438 and *ibid.* 675;
   G. Altarelli and G. Parisi, Nucl. Phys. **B126** (1977) 298.
6. F. Halzen and A. Martin, "Quarks and Leptons", John Wiley and Sons 1984.
7. E.A. Kuraev, L.N. Lipatov and V.S. Fadin, Sov. Phys. JETP **45** (1977) 199;
   Ya.Ya. Balitsky and L.N. Lipatov, Sov. J. Nucl. Phys. **28** (1978) 822;
   L.N. Lipatov, Sov. Phys. JETP **63** (1986) 904.
8. J. Forshaw and D. Ross, "QCD and the Pomeron", Cambridge Univ. Press 1997.
9. M. Ciafaloni, Nucl. Phys. **B296** (1987) 249;
   S. Catani, F. Fiorani and G. Marchesini, Phys. Lett. **B234** (1990) 339 and Nucl. Phys. **B336** (1990) 18.
10. F. Zomer, these proceedings.
11. A.H. Mueller, Nucl. Phys. **B** (Proc. Suppl.) **18C** (1991) 125.
12. J. Bartels, V. Del Duca, A. De Roeck, D. Graudenz and M. Wusthoff, Phys. Lett. **B384** (1996) 300.
13. G. Ingelman, Proc. of the HERA workshop, Ed.s W. Buchmüller and G. Ingelman, Hamburg 1992, Vol. 3, p. 1366.
14. H. Jung, Comp. Phys. Comm. **86** (1995) 147.
15. G. Marchesini, B.R. Webber, G. Abbiendi, I.G. Knowles, M.H. Seymour and L. Stanco, Comp. Phys. Comm. **67** (1992) 465.
16. L. Lönnblad, Comp. Phys. Comm. **71** (1992) 15.
17. B. Andersson, G. Gustafson and L. Lonnblad, Nucl. Phys. **B339** (1990) 393.
18. H. Kharraziha and L. Lönnblad, JHEP **03** (1998) 006.
19. G.P. Salam, JHEP **03** (1999) 009.
20. T. Sjöstrand, Comp. Phys. Comm. **82** (1994) 74.
21. J. Huth *et al.*, Proc. of the 1990 DPF Summer Study on High Energy Physics, Snowmass, Colorado, Ed. E.L. Berger (World Scientific, Singapore, 1992) p. 134;
    F. Abe *et al.* [CDF Collaboration], Phys. Rev. **D45** (1992) 1448.
22. J. Breitweg *et al.* [ZEUS Collaboration], Eur. Phys. J. **C6** (1999) 239.
23. C. Adloff *et al.* [H1 Collaboration], Nucl. Phys. **B538** (1999) 3.
24. J.G. Contreras Nuno, unpublished Ph.D. thesis, Dortmund University, 1997.
25. S. Catani and M.H. Seymour, Nucl. Phys. **B485** (1997) 291.

26. J. Outhwaite, these proceedings.
27. V.S. Fadin and L.N. Lipatov, Phys. Lett. **B429** (1998) 127.
28. D.A. Ross, Phys. Lett. **B431** (1998) 161.
29. G.P. Salam, JHEP **07** (1998) 019.
30. J.R. Forshaw, D.A. Ross and A.S. Vera, Phys. Lett. **B455** (1999) 273.
31. N. Armesto, J. Bartels and M.A. Braun, Phys. Lett. **B442** (1998) 459.
32. J. Kwiecinski, A.D. Martin and J.J. Outhwaite, Eur. Phys. J. **C9** (1999) 611.
33. C. Adloff *et al.* [H1 Collaboration], Phys. Lett. **B462** (1999) 440.
34. C. Adloff *et al.* [H1 Collaboration], hep-ex/9812024.
35. G. Kramer and B. Pötter, Phys. Lett. **B453** (1999) 295;
36. B. Pötter, these proceedings.